Redox Properties of Mesophilic and Hyperthermophilic Rubredoxins as a Function of Pressure and Temperature†

Laurent D. Gillès de Pélichy‡ and Eugene T. Smith*,§

Department of Chemistry, Florida Institute of Technology, Melbourne, Florida 32901-6988, and Department of Chemistry, Hamline University, St. Paul, Minnesota 55104

Received February 9, 1999

ABSTRACT: The formal equilibrium reduction potentials of recombinant electron transport protein, rubredoxin (MW = 7500 Da), from both the mesophilic *Clostridium pasteurianum* (T_{opt} = 37 °C) and hyperthermophilic *Pyrococcus furiosus* (T_{opt} = 95 °C) were recorded as a function of pressure and temperature. Measurements were made utilizing a specially designed stainless steel electrochemical cell that easily maintains pressures between 1 and 600 atm and a temperature-controlled cell that maintains temperatures between 4 and 100 °C. The reduction potential of *P. furiosus* rubredoxin was determined to be 31 mV at 25 °C and 1 atm, −93 mV at 95 °C and 1 atm, and 44 mV at 25 °C and 400 atm. Thus, the reduction potential of *P. furiosus* rubredoxin obtained under standard conditions is likely to be dramatically different from the reduction potential obtained under its normal operating conditions. Thermodynamic parameters associated with electron transfer were determined for both rubredoxins (for *C. pasteurianum*, $\Delta V° = -27$ mL/mol, $\Delta S° = -36$ cal K^{-1} mol^{-1}, and $\Delta H° = -10$ kcal/mol, and for *P. furiosus*, $\Delta V° = -31$ mL/mol, $\Delta S° = -41$ cal K^{-1} mol^{-1}, and $\Delta H° = -13$ kcal/mol) from its pressure− and temperature−reduction potential profiles. The thermodynamic parameters for electron transfer ($\Delta V°$, $\Delta S°$, and $\Delta H°$) for both proteins were very similar, which is not surprising considering their structural similarities and sequence homology. Despite the fact that these two proteins exhibit dramatic differences in thermostability, it appears that structural changes that confer dramatic differences in thermostability do not significantly alter electron transfer reactivity. The experimental changes in reduction potential as a function of pressure and temperature were simulated using a continuum dielectric electrostatic model (DELPHI). A reasonable estimate of the protein dielectric constant ($\epsilon_{protein}$) of 6 for both rubredoxins was determined from these simulations. A discussion is presented regarding the analysis of electrostatic interaction energies of biomolecules through pressure- and temperature-controlled electrochemical studies.

The ocean, a diverse habitat spanning a wide range of pressures and temperatures, contains more than half of the world's biosphere. Many marine organisms flourish at depths of >4000 m at pressures of >400 atm (*1*), conditions sufficient to inhibit growth in nonadapted microorganisms (*2*). Hyperthermophilic microorganisms, including *Pyrococcus furiosus*, have been isolated near hydrothermal vents at these great depths, and at temperatures exceeding 100 °C (*3*−*5*). In the past several decades since their first isolation, considerable progress has been made in elucidating their unusual biochemical pathways, although it is far from understood how these unusual organisms are able to thrive in such an extreme environment.

Electron transport chains are an important pathway by which virtually all living organisms, including hyperthermophiles, obtain energy. In this study, we investigate the role of pressure and temperature on this fundamental process. It has been previously determined that the electron transfer properties of hyperthermophiles are dramatically influenced by temperature (*6*−*9*). For instance, the reduction potentials of *P. furiosus* rubredoxin (−1.4 mV/°C up to 70 °C; *6*) and ferredoxin (−1.7 mV/°C; *7*) were found to be temperature-dependent as determined by potentiometric EPR titrations. Rubredoxin serves as an ideal model for investigating the role of pressure and temperature on biological electron transfer since it is a relatively simple electron transfer protein (MW = 7500 Da), and it has been isolated from a number of microorganisms that grow over a broad temperature range. The primary and tertiary structures have also been determined for a number of microbial rubredoxins (*10*). In this study, we present electrochemical results as a function of pressure and temperature for both mesophilic *Clostridium pasteurianum* and hyperthermophilic *P. furiosus* rubredoxins. In addition, we discuss the implications at a molecular level of pressure- and temperature-dependent reduction potentials.

While pressure- and temperature-dependent reduction potentials have been reported for a number of proteins (*11*, *12*), few studies have been aimed at understanding these observed changes at a molecular level (*13*−*15*). It has long been recognized that electrostatic interactions are an important determinant of enzymatic and electron transfer reactivity. In simple terms, Coulombic interaction energies, which

† This research was supported by Grant GM 50736 from the National Institutes of Health.

* To whom correspondence should be addressed: Department of Chemistry, Hamline University, 1536 Hewitt Ave., St. Paul, MN 55104. Phone: (651) 523-2283. Fax: (651) 523-2620. E-mail: gsmith@gw.hamline.edu.

‡ Florida Institute of Technology.

§ Hamline University.

10.1021/bi990322j CCC: $18.00
Published on Web 05/26/1999

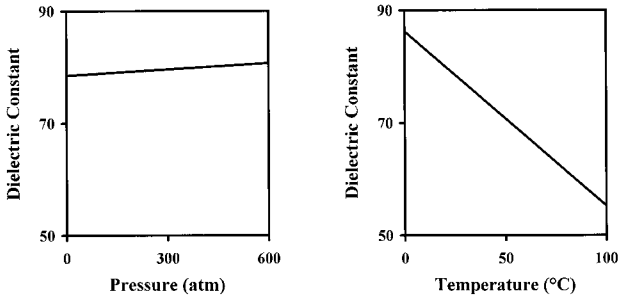

FIGURE 1: Dielectric constant of water as a function of pressure and temperature (*17*).

contribute to the magnitude of the reduction potential, are directly related to the magnitude of charge and inversely related to the distance between charges and the screening of the medium. Coulombic interaction energies between two charged particles *i* and *j* in a homogeneous medium can be calculated as follows:

$$E = q_i q_j / \epsilon_{ij} r_{ij} \quad (1)$$

where q is the charge, ϵ is the dielectric constant, and r is the distance between the two charges. Electrostatic interaction energies are much more difficult to determine for biomolecules that contain numerous charge groups that are immersed in media with different dielectric constants. In typical macroscopic continuum models for proteins (*16*), distances between atoms (r) are determined from X-ray crystal structures, atomic partial charges (q) are assigned to individual atoms on the basis of molecular mechanical simulations, and a dielectric constant is assigned to both the protein ($\epsilon_{protein}$) and solvent ($\epsilon_{solvent}$).

In the past, the magnitude of the charge (q) and the distance between charges (r) have been traditionally perturbed through molecular biology approaches (e.g., site mutations) or chemical modification to investigate the role of electrostatic interaction energies in proteins. Despite the progress in this area, we are still far from understanding the fundamental role of electrostatic interactions in proteins. In this study, we present a novel approach that provides additional insight into the role of electrostatic interactions in proteins through the analysis of equilibrium reduction potentials as a function of pressure and temperature. In this new approach, pressure and temperature are used to perturb the dielectric constant (ϵ) of both the protein and solvent.

Both pressure− and temperature−reduction potential profiles provide important information about electrostatic interaction energies in proteins. As illustrated in Figure 1, the dielectric constant of water increases as a function of pressure and decreases as a function of temperature. Thus, as temperature is increased or pressure is decreased, the level of ordering or shielding of the solvent molecules around a charged electron transfer center decreases and hence charged atoms are "felt" more strongly near the electron transfer center. It would be expected that at high temperatures or low pressures, it would require more work to bring an electron to an electron transfer center that is surrounded by atoms with a net negative charge. The change in the amount of work required to bring an electron to the electron transfer center, through the perturbation of the dielectric constant of the medium, is reflected in the experimentally measured formal equilibrium reduction potential ($E^{\circ\prime}$).

Formal equilibrium reduction potentials represent an important aspect in the thermodynamic analysis of biological electron transfer reactions. This parameter has been measured for many electron transfer proteins using a variety of voltammetric methods and various modified and unmodified solid electrode surfaces (*18*−*20*). Advantages of direct electrochemical methods include low cost, rapidity and nondestructive nature of the measurements, and small sample volume and low concentration requirements. To further our understanding of biological electron transfer reactions, electrochemical cells were specifically designed to measure equilibrium reduction potentials as a function of pressure (*13*) and temperature (*21*). These pressure- and temperature-controlled electrochemical experiments provide important information concerning the role of protein−solvent interactions on electron transfer, as well as information concerning changes in electrostatic interaction energies of electron transport proteins.

MATERIALS AND METHODS

Protein Sources. Escherichia coli strains BL21-DE3 (Novagen, Inc.) containing plasmids with synthetic genes with wild-type sequences of either *C. pasteurianum* or *P. furiosus* rubredoxins were grown in LB medium supplemented with ampicillin (50 μg/mL) at 38 °C in a shaker water bath (*22*). M. K. Eidsness, D. M. Kurtz, Jr., and R. A. Scott (Department of Chemistry and Center for Metalloenzyme Studies, University of Georgia, Athens, GA) generously supplied both strains. At an optical density of 0.6−0.8 at 600 nm, 0.9 g/L isopropyl β-D-thiogalactoside (IPTG) and 1 g/L ferrous sulfate were added to the medium. The cultures were shaken for an additional 4 h at 38 °C and then harvested by centrifugation. The cell pellets were resuspended, sonicated, and centrifuged, and the rubredoxin was purified by ion exchange and size exclusion chromatography. The purity was determined by UV−visible spectroscopy as previously described ($A_{494nm}/A_{280nm} > 0.36$; *10*).

Electrochemistry. The cross-section view of the pressure-controlled stainless steel electrochemical cell is shown in Figure 2A (*13*). This electrochemical cell was designed and tested to maintain an anaerobic sample at pressures from 1 to 600 atm and temperatures from 4 to 100 °C. Additional improvements were made to the original electrochemical cell design (*13*). An electrical contact with the counter and reference electrode was redesigned to minimize the compression of the Delrin sheath (see Figure 2B). Despite these changes, the Delrin components that insulated the electrodes (d and l) needed to be replaced every other experimental run due to their compression at high pressures. A vice purchased from a local hardware store was used instead of a hydraulic jack to minimize problems with drifting in the pressure measurements. Last, the sample injection port was replaced with a tiny bolt to ensure that no leaking occurred at high pressures.

A 2.0 mL solution containing 0.5 mM recombinant *C. pasteurianum* or *P. furiosus* rubredoxin in 25 mM phosphate (pH 6.7) and 0.05 M $MgCl_2$ as an electrode promoter in a stoppered 8 mL vial was made anaerobic by cycling between a vacuum and nitrogen gas. The sample and reference solution (0.100 M NaCl) were then transferred under anaerobic conditions using an anaerobic glovebox into the

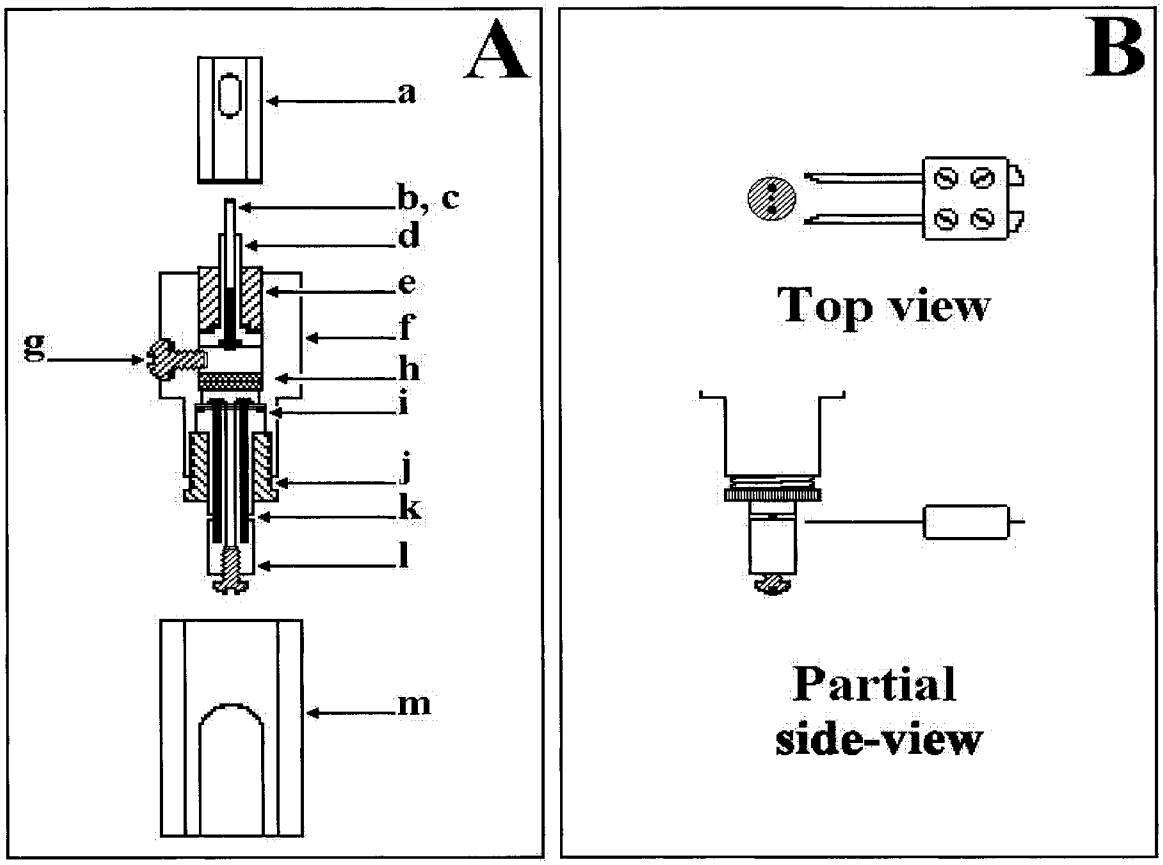

FIGURE 2: (A) Cross section of the pressure-controlled electrochemical cell showing the upper jacking component (a), the stainless steel rod (b) with pyrolytic graphite working electrode (c, illustrated in black), the upper Delrin sheath (d), the stainless steel piston (e), the cell body (f), the sample port (g), stainless steel frits (h), the stainless steel retaining ring (i), the threaded brass fitting (j), the Ag/AgCl reference and counter electrodes (k, illustrated in black), the lower Delrin sheath with a reference solution port (l), and the lower jacking component (m) (modified from ref *13*). (B) Top and partial side view of the pressure-controlled cell showing the electrical connections to counter and reference electrodes. The lower Delrin sheath in the partial side view has been rotated 90° along its vertical axis relative to its position as illustrated in panel A (component l).

appropriate sample compartment of the electrochemical cell, avoiding the introduction of gas bubbles. The entire assembly was placed within a vise, and a load was applied and monitored via a load cell as previously described (*13*). The applied pressure was calculated by dividing the load by the known surface area of the piston, and converted to units of atmospheres. The temperature was maintained utilizing a circulating water bath via a ported stainless steel water jacket (*13*), or by using a temperature-controlled electrochemical cell as previously described (*21*). While both electrochemical cells can be used to obtain temperature-controlled voltammograms, the sample can be visually monitored for denaturation in the earlier cell design (*21*), and the potential of the saturated Ag/AgCl reference electrode as a function of temperature has been well-established.

Reduction potentials were determined by direct electrochemistry, a method that entails the unmediated interfacial reduction and reoxidation of an electron transfer molecule at an electrode surface. At least two cyclic voltammograms were recorded at each pressure and temperature utilizing a CV-50W BAS potentiostat. Cyclic voltammograms were determined to be reversible at scan rates of <30 mV/s, and scan rates from 5 to 30 mV/s were used throughout the study. Reduction potentials from each cyclic voltammogram were determined from the midpoint between the anodic and cathodic peak potentials. All reduction potentials were normalized for pressure and temperature as previously described (*13*) and reported versus the SHE.[1] Thermodynamic parameters associated with electron transfer were calculated from the electrochemical experiments described above according to the following equations:

$$\Delta V^\circ = -nF(\partial E^\circ/\partial P)_T \quad (2)$$

$$\Delta S^\circ = nF(\partial E^\circ/\partial T)_P \quad (3)$$

$$\Delta H^\circ = -nF[\partial(E^\circ/T)/\partial(1/T)]_P \quad (4)$$

where ΔV°, ΔS°, and ΔH° are the standard molar volume, standard reaction entropy, and standard reaction enthalpy, respectively.

Electrostatic Calculations. It has been proposed (*13*, *14*) that pressure- and temperature-induced changes in the reduction potential $[(\Delta E/\Delta P)_T$ or $(\Delta E/\Delta T)_P]$ can be attributed to changes in atomic partial charges, charge separation, or charge environment according to the following equations:

$$(\Delta E/\Delta P)_\mathrm{T} = [\Delta(\sum q_i q_j/\epsilon_{ij} r_{ij})/\Delta P]_T \quad (5)$$

$$(\Delta E/\Delta T)_\mathrm{P} = [\Delta(\sum q_i q_j/\epsilon_{ij} r_{ij})/\Delta T]_P \quad (6)$$

All of these parameters are likely to be influenced by pressure and temperature to various degrees, but experimental evi-

[1] Abbreviations: SHE, standard hydrogen electrode.

dence suggests that electronic charge and charge separation are not as likely to be as pressure- and temperature-dependent as the dielectric constant (*13*). On the basis of these assumptions, the dielectric constants of the solvent and protein were changed as described below to simulate pressure and temperature changes.

Changes in reduction potential as a function of pressure and temperature were calculated using the continuum macroscopic electrostatic model (DELPHI, 1989, Columbia University, New York). This macroscopic model treats the electrical properties of the solvent and protein as distinct continuums, visualizing the protein as a low-ϵ "cavity" embedded in a solvent medium with a higher value of ϵ. The average electrical properties of a protein are approximated by the internal protein dielectric constant, $\epsilon_{protein}$. This continuum dielectric model is particularly attractive in that it is able to model with reasonable accuracy the electrical properties of the solvent, $\epsilon_{solvent}$, including solutions with different ionic strengths. Moreover, this model in conjunction with a finite-difference technique accounts for the complex structure of proteins at a microscopic level. On the basis of its X-ray crystal structure, a protein is mapped onto a three-dimensional grid, partial atomic charges and dielectric constants are assigned to points on the grid, and the potential energy of the grid is calculated utilizing a numerical solution to the Poisson−Boltzmann equation.

Atomic partial charges were assigned for amino acids (*23*) and the FeS_4 center (*24*). Spatial arrangement of atomic charges were assigned as determined from X-ray crystal structures of the proteins (25 for *C. pasteurianum* rubredoxin and 26 for *P. furiosus* rubredoxin). The value of the dielectric constant of water was assigned as a function of pressure and temperature as shown in Figure 1. The value for the protein dielectric constant was varied (see Results and Discussion). In this unique application of DELPHI, the dielectric constants of the solvent and protein are varied to reproduce changes in the reduction potential of rubredoxins as a function of pressure and temperature. For example, the calculated net change in electrostatic energy is the difference in energy between two temperatures, represented by different dielectric constants for the solvent and protein, and the difference in energy between both oxidation states. Thus, the calculated net change in electrostatic energy represents a $[\Delta(\Delta G)]$ converted to units of millivolts.

RESULTS AND DISCUSSION

Influence of Pressure on Reduction Potentials. Representative cyclic voltammograms of *C. pasteurianum* rubredoxin at two pressures and the reduction potential of *C. pasteurianum* rubredoxin as a function of pressure are shown in panels A and B of Figure 3, respectively. The reduction potentials of both *C. pasteurianum* and *P. furiosus* rubredoxins were determined to be linearly pressure-dependent, 0.028 and 0.033 mV/atm, respectively. Both proteins have negative standard molar volumes ($\Delta V°$), which were calculated from eq 2, and they are listed in Table 1. This indicates that the oxidized state of the electron transfer center, $[FeS_4]^-$, is more stable than the reduced state, $[FeS_4]^{2-}$, at lower pressures. This observation can be rationalized in simple electrostatic terms. The dielectric constant of water ($\epsilon_{solvent}$) is lower at lower pressures as illustrated in Figure 1A. Since a species with a lower net negative charge would be more stable in a medium with a lower dielectric constant, it would be expected that the oxidized protein is more stable at lower pressures.

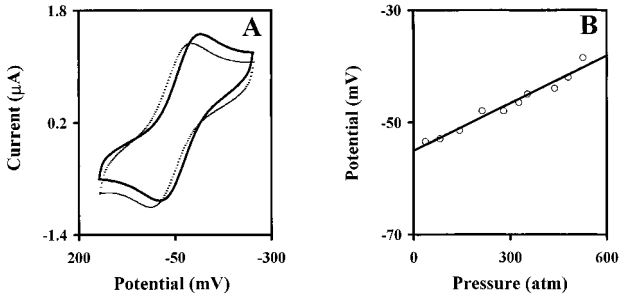

FIGURE 3: (A) Cyclic voltammograms of 0.5 mM *C. pasteurianum* rubredoxin in 25 mM phosphate (pH 6.7) recorded at 84 atm (solid line) and 536 atm (dashed line), 25 °C, and a scan rate of 5 mV/s. (B) Reduction potential of *C. pasteurianum* rubredoxin as a function of pressure.

Table 1: Thermodynamic Parameters Associated with Electron Transfer of Rubredoxin

	C. pasteurianum	*P. furiosus*
$E°'$ at 25 °C and 1 atm (mV)	−55	31
$\Delta V°$ (mL/mol)	−27	−31
$\Delta S°$ (cal K^{-1} mol^{-1})	−36	−41
$\Delta H°$ (kcal/mol)	−10	−13

Electrostatic Calculations as a Function of Pressure. It is established from the data presented in Figure 3B that pressure influences electron transfer equilibrium. A key issue to be resolved now is the rationalization at a molecular level of the direction and magnitude of experimentally observed changes in reduction potential. The continuum dielectric model (DELPHI) was used to reproduce changes in the reduction potential of rubredoxin as function of pressure. This electrostatic model calculates changes in electrostatic interaction energies, which can be converted to changes in reduction potential, based on differences in charge (q), charge separation (r), and the dielectric constant (ϵ). The dielectric constant of water is known as a function of pressure (Figure 1A), and the dielectric constant of rubredoxin was assigned in the calculations as described below.

Protein Dielectric Constant as a Function of Pressure. The dielectric constant of water does not change significantly as a function of pressure from 1 to 600 atm ($\Delta\epsilon_{solvent} < 4\%$; see Figure 1A). It has been previously assumed that the dielectric constant of a protein is low ($\epsilon_{protein} < 4$) since the reorientation of its dipoles in response to an electric field is highly restricted (*27*, *28*). Therefore, the dielectric constant of a protein would be expected to be even less pressure-dependent than that of a polar solvent such as water (i.e., $\Delta\epsilon_{protein} \ll 4\%$ from 1 to 600 atm). Therefore, it was assumed in our calculations that the protein dielectric constant ($\epsilon_{protein}$) was pressure-independent from 1 to 600 atm.

The calculated change in reduction potential of *C. pasteurianum* rubredoxin as a function of pressure for different values of the pressure-independent protein dielectric constant ($\epsilon_{protein}$) is shown in Figure 4. The dashed line in this figure represents the experimentally observed value ($dE°'/dP = 0.028$ mV/atm). It is seen from this figure that the experimental results cannot be reproduced using low values for the dielectric constant ($\epsilon_{protein} < 4$). Relatively large negative

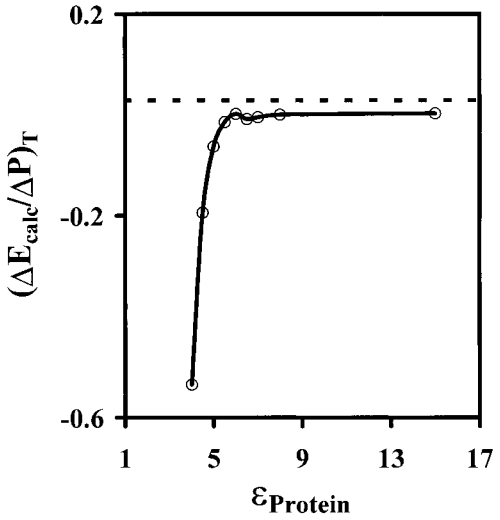

FIGURE 4: Calculated change in reduction potential of *C. pasteurianum* rubredoxin as a function of pressure for different values of the protein dielectric constant. See the text for details of the calculations.

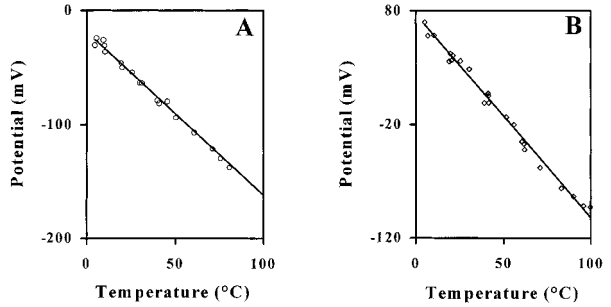

FIGURE 5: Reduction potential of *C. pasteurianum* (A) and *P. furiosus* (B) rubredoxin as a function of temperature. Symbols denote experimental points, and the solid line represents the simulation based on dielectric constants as described in text.

changes in the reduction potential are predicted for small changes in pressure at these low dielectric constants. Little change in the reduction potential as a function of pressure ($dE^{\circ\prime}/dP = 0.002$ mV/atm) is predicted for rubredoxin for large values of the dielectric constant ($\epsilon_{protein} \geq 6$). Thus, a reasonable estimate of the protein dielectric constant $\epsilon_{protein}$ is 6. Similar results as illustrated in Figure 4 were also obtained for *P. furiosus* rubredoxin [results not shown, $(dE^{\circ\prime}/dP)_{observed} = 0.033$ mV/atm and $(dE^{\circ\prime}/dP)_{calcd} = 0.001$ mV/atm for an $\epsilon_{protein}$ of ≥ 6].

Influence of Temperature and Reaction Entropies. The reduction potentials of both *C. pasteurianum* and *P. furiosus* (see Figure 5) rubredoxins were determined to be linearly temperature-dependent (−1.6 and −1.8 mV/°C, respectively). The latter value is comparable to the value determined for *P. furiosus* rubredoxin by spectroelectrochemistry (−1.4 mV/°C up to 70 °C; *6*). The standard entropies for *C. pasteurianum* and *P. furiosus* rubredoxin calculated using eq 3 were determined to be similar (see Table 1). These values were significantly more negative than those reported for other mesophilic electron transfer proteins ($\Delta S^\circ = -2$ to -16 eu; *11*) but similar to values reported for other hyperthermophilic proteins ($\Delta S^\circ = -28$ to -60 eu; *9*). Both *C. pasteurianum* and *P. furiosus* rubredoxins have negative standard entropies (ΔS°), indicating that the oxidized state of the electron transfer center, $[FeS_4]^-$, is more stable than the reduced state, $[FeS_4]^{2-}$, at higher temperatures. This observation can be rationalized in simple electrostatic terms. The dielectric constant of water ($\epsilon_{solvent}$) is lower at higher temperatures as illustrated in Figure 1B. Since a species with a lower net negative charge would be more stable in a medium with a lower dielectric constant, it would be expected that the oxidized protein would be more stable at higher temperatures.

Reaction Enthalpies ($\Delta H^{\circ\prime}$). The standard reaction enthalpies of *C. pasteurianum* and *P. furiosus* rubredoxins were calculated from eq 4, and they are listed in Table 1. These values are within the range of values reported for other hyperthermophilic electron transfer proteins (*9*). The standard reaction enthalpy for both proteins was negative, indicating that reduction is exothermic. On the basis of Le Châtlier's principle, the concentration of the oxidized species would be expected to increase as the temperature increases. Interestingly, both the enthalpy and entropy terms contribute to the preferential formation of the oxidized species at elevated temperatures.

Electrostatic Calculations as a Function of Temperature. It is clear from the data presented in Figure 5 that temperature also influences the electron transfer equilibrium. As discussed above for pressure-dependent reduction potentials, a key issue to be resolved is the rationalization at a molecular level of the direction and magnitude of experimentally observed changes in reduction potential. The dielectric continuum model (DELPHI) was likewise used to reproduce changes in the reduction potential of rubredoxin as a function of temperature using appropriate values of the dielectric constant for the solvent and protein. The dielectric constant of water is known as a function of temperature (Figure 1B), and the dielectric constant of rubredoxin was assigned as described below.

Protein Dielectric Constant as a Function of Temperature. The dielectric constant of water is known to change appreciably from 5 to 100 °C ($\Delta\epsilon_{solvent} > 30\%$; see Figure 1B). The dielectric constant of a protein cannot be readily measured, and it cannot be assumed to be temperature-independent (*29*). It is known that pure nonpolar solvents have temperature-dependent dielectric constants, but they are not as temperature-dependent as water (*17*). We propose that a reasonable value of the protein dielectric constant can be estimated from the information obtained from pressure-controlled electrochemical experiments and the simulations of these data. As discussed above, the protein dielectric constant is likely to be pressure-independent. Thus, the value of the protein dielectric constant ($\epsilon_{protein} = 6$) that reasonably reproduced the room-temperature pressure-induced changes in the reduction potential of *C. pasteurianum* rubredoxin was then used to reproduce the temperature-induced changes in its reduction potential. The value of the protein dielectric constant was changed as a function of temperature to reproduce the experimental observations shown in Figure 5. Similar calculations have been performed by our group to reproduce reduction potentials of other electron transfer proteins as a function of temperature (*29*). These earlier calculations, however, did not include an estimate of the protein dielectric constant based on information obtained from pressure-induced changes in the reduction potential.

Both the experimental reduction potentials of *C. pasteurianum* and *P. furiosus* rubredoxin as a function of temperature (see Figure 5) were reproduced using $d\epsilon_{protein}/dT =$

-0.005 and -0.010 °C^{-1}, respectively, over a temperature range from 5 to 100 °C. A protein dielectric constant $\epsilon_{protein}$ of 6 at 25 °C was used for both proteins. The $d\epsilon_{protein}/dT$ of *P. furiosus* rubredoxin was greater, which suggests that the actual protein dielectric constant is likely to be slightly higher than that of *C. pasteurianum* rubredoxin. In comparison, $d\epsilon/dT = -0.324$ and -0.002 °C^{-1} for water and benzene, respectively (*17*, *30*). Thus, the observed changes in the protein dielectric constant with temperature are reasonable for a medium that is believed to have a low dielectric constant.

Thermodynamic Considerations. The thermodynamic parameters for electron transfer ($\Delta V°$, $\Delta S°$, and $\Delta H°$) for both proteins were very similar, which is not surprising considering their structural similarities and sequence homology (*26*). These parameters for both proteins indicate that the formation of $[FeS_4]^-$ is favored at high temperatures and low pressures, which is consistent with the electrostatic calculations. Remarkably, the two proteins exhibit dramatic differences in thermostability. *P. furiosus* rubredoxin remains essentially undenatured after incubation at 95 °C for more than 24 h, whereas *C. pasteurianum* rubredoxin is rapidly denatured at 80 °C (*6*). On the basis of the data presented in Table 1, it appears that structural changes that confer dramatic differences in thermostability do not dramatically alter electron transfer reactivity. It is noted that the reaction volume ($\Delta V°$) is slightly more negative, the reaction entropy ($\Delta S°$) is slightly more negative, and the reaction enthalpy ($\Delta H°$) is more exothermic for *P. furiosus* rubredoxin. These parameters suggest that the oxidized state, which has a lower net negative charge, is slightly more stable than the reduced state of the protein when compared to the different oxidation states of *C. pasteurianum* rubredoxin. In general, we predict that in most cases, standard reaction volumes ($\Delta V°$) and standard reaction entropies ($\Delta S°$) of electron transfer proteins will have the same sign because they both are a measure of the differences in stability of each oxidation state.

Electrostatic Considerations. Both rubredoxins have reduction potentials that decreased as the pressure decreased (see Figure 3B) or the temperature increased (see Figure 5). This inverse relationship between the slopes of pressure− and temperature−reduction potential profiles has previously been noted for cytochrome *c* (*14*). Interestingly, these inverse changes in reduction potential with pressure and temperature appear to follow the same trend as the dielectric constant of the solvent (see Figure 1). At a macroscopic level, reduction potentials reflect the changes in electrostatic interaction energies resulting from changes in pressure and temperature. Changes in reduction potential observed in both pressure-controlled (*12*, *31*) and temperature-controlled (*11*, *32*) electrochemical experiments are thought to result from differences in solvent−solute interactions between oxidation states of an electron transfer molecule. The stability of each oxidation state is dependent on the ability of protein−solvent interactions to neutralize excess charge as a function of pressure and temperature. At low pressures or high temperatures, the solvent dielectric constant is lower (see Figure 1), and therefore, the solvent is less efficient at solvating excess charge. To a lesser extent, the protein dielectric constant will also decrease as the temperature increases. Thus, the oxidation state with the least amount of excess charge is more likely to be the most stable at low pressures or elevated temperatures.

An accurate representation of the protein−solvent interface is a significant challenge for any electrostatic model used to reproduce experimentally observed changes in reduction potential. The continuum dielectric model (DELPHI) has had reasonable success at reproducing these changes (*33*). Recently, quantum mechanical calculations have revealed that the net surface charge of a protein may be transferred to the solvent, and this charge transfer across the protein−water interface is likely to be significant (*34*). An important consequence of changes in solvent−solute interactions induced by pressure or temperature is that the electrostatic environment of a redox center is perturbed. These changes alter the electrostatic interaction energy between atoms in a protein, which determines the reduction potential.

Additional Consequence of Pressure- and Temperature-Dependent Reduction Potentials. When the thermodynamics of electron transport pathways are being considered, it is equally important to consider the relevant operating conditions of the electron transfer proteins. Pressure- and temperature-controlled electrochemical experiments with electron transfer proteins allow for thermodynamic measurements to be made under more relevant experimental conditions, specifically their normal operating conditions. For example, in this study, it was determined that the rubredoxin isolated from *P. furiosus*, which grows at 95 °C and 400 atm, has an $E°'$ of 31 mV at room temperature and atmospheric pressure, an $E°'$ of -93 mV at 95 °C and atmospheric pressure, and an $E°'$ of 44 mV at room temperature and 400 atm. Although not measured in this study, the reduction potential of *P. furiosus* rubredoxin is predicted to be around -80 mV at 95 °C and 400 atm. The potential of the reference electrode at 95 °C and 400 atm needs to be determined to report the reduction potential of *P. furiosus* rubredoxin versus the SHE, and these experiments are currently in progress.

CONCLUSIONS

An abundance of electrostatic information is obtained from pressure- and temperature-controlled electrochemical experiments that are not available through a single room-temperature measurement. Electrochemical experiments with other rubredoxin variants as a function of pressure and temperature should provide further support that electrostatic interactions play an important role in determining the reduction potential of a protein as previously suggested (*13*, *14*).

REFERENCES

1. Gross, M., and Jaenicke, R. (1994) *Eur. J. Biochem. 221*, 617−630.
2. ZoBell, C. E. (1970) in *High-Pressure Effects on Cellular Processes* (Zimmerman, A. M., Ed.) pp 85−130, Academic Press, New York.
3. Stetter, K. O. (1986) in *The Thermophiles: General, Molecular and Applied Microbiology* (Brock, T. D., Ed.) pp 39−74, Wiley, New York.
4. Stetter, K. O., Fiala, G., Huber, G., Huber, R., and Segerer, G. (1990) *FEMS Microbiol. Rev. 755*, 117−124.
5. Adams, M. W. W. (1990) *FEMS Microbiol. Rev. 75*, 219−238.
6. Adams, M. W. W. (1992) *Adv. Inorg. Chem. 38*, 341−396.
7. Park, J. B., Fan, C., Hoffman, B. M., and Adams, M. W. W. (1991) *J. Biol. Chem. 266*, 19351−19356.
8. Smith, E. T., Blamey, J., and Adams, M. W. W. (1993) *Curr. Sep. 12*, 131−134.

9. Smith, E. T., Blamey, J., Zhou, Z. H., and Adams, M. W. W. (1995) *Biochemistry 34*, 7161−7169.
10. Blake, P. R., Park, J.-B., Zhou, Z. H., Hare, D. R., Adams, M. W. W., and Summers, M. F. (1992) *Protein Sci. 1*, 1508−1521.
11. Taniguchi, V. T., Sailasuta-Scott, N., Anson, F. C., and Gray, H. B. (1980) *Pure Appl. Chem. 52*, 2275−2281.
12. Cruañes, M. T., Rodgers, K. K., and Sligar, S. G. (1992) *J. Am. Chem. Soc. 114*, 9660−9661.
13. Smith, E. T. (1995) *Anal. Biochem. 224*, 180−186.
14. Smith, E. T. (1995) *J. Am. Chem. Soc. 117*, 6717−6719.
15. Swartz, P. D., and Ichiye, T. (1996) *Biochemistry 35*, 13772−13779.
16. Honig, B. H., Hubbell, W. L., and Flewelling, R. F. (1986) *Annu. Rev. Biophys. Biophys. Chem. 15*, 163−193.
17. Weast, R. C., Ed. (1986) *Handbook of Chemistry and Physics*, 66th ed., CRC Press, Boca Raton, FL.
18. Frew, J. E., and Hill, H. A. O. (1988) *Eur. J. Biochem. 172*, 261−269.
19. Armstrong, F. A., Hill, H. A. O., and Walton, N. J. (1988) *Acc. Chem. Res. 21*, 407−413.
20. Armstrong, F. A. (1990) *Struct. Bonding (Berlin) 72*, 137−221.
21. Smith, E. T., and Adams, M. W. W. (1992) *Anal. Biochem. 207*, 94−99.
22. Eidness, M. K., Richie, K. A., Burden, A. E., Kurtz, D. M., Jr., and Scott, R. A. (1997) *Biochemistry 36*, 10406−10413.
23. Cornell, W. D., Cieplak, P., Bayly, C. I., Gould, I. R., Merz, K. M., Ferguson, D. M., Spellmeyer, D. C., Fox, T., Caldwell, J. W., and Kollman, P. A. (1995) *J. Am. Chem. Soc. 117*, 5179−5198.
24. Noodleman, L., Norman, H. G., Osborne, J. H., Aizman, A., and Case, D. (1985) *J. Am. Chem. Soc. 107*, 3418−3426.
25. Watenpaugh, K. D., Sieker, L. C., and Jensen, L. H. (1980) *J. Mol. Biol. 138*, 615.
26. Day, M. W., Hsu, B. T., Joshua-Tor, L., Park, J.-B., Zhou, Z. H., Adams, M. W. W., and Rees, D. C. (1992) *Protein Sci. 1*, 1494−1507.
27. Gilson, M. K., and Honig, B. H. (1986) *Biopolymers 25*, 2097−2119.
28. Gilson, M. K., and Honig, B. H. (1987) *Nature 330*, 15−17.
29. Christen, R. P., Nomikos, S. I., and Smith, E. T. (1996) *J. Bioinorg. Chem. 6*, 515−522.
30. Washburn, E. W., Ed. (1926) *International Critical Tables*, Vol. 6, McGraw-Hill, New York.
31. Cruañes, M. T., Drickamer, H. G., and Faulkner, L. R. (1992) *J. Phys. Chem. 96*, 9888−9892.
32. Hupp, J. T., and Weaver, M. J. (1984) *Inorg. Chem. 23*, 3639−3644.
33. Rogers, K. K., and Sligar, S. G. (1991) *J. Am. Chem. Soc. 113*, 9419−9421.
34. Nadig, G., Van Zant, L. C., Dixon, S. L., and Merz, K. M., Jr. (1998) *J. Am. Chem. Soc. 120*, 5593−5594.

BI990322J